

See discussions, stats, and author profiles for this publication at: <https://www.researchgate.net/publication/263942712>

# Sulfonamide Molecular Crystals: Structure, Sublimation Thermodynamic Characteristics, Molecular Packing, Hydrogen Bonds Networks

ARTICLE in CRYSTAL GROWTH & DESIGN · JULY 2013

Impact Factor: 4.89 · DOI: 10.1021/cg400666v

---

CITATIONS

9

---

READS

30

## 5 AUTHORS, INCLUDING:



[German L Perlovich](#)

Institute of Solution Chemistry of RAS

142 PUBLICATIONS 1,479 CITATIONS

[SEE PROFILE](#)



[Lars Kr. Hansen](#)

University of Tromsoe

41 PUBLICATIONS 233 CITATIONS

[SEE PROFILE](#)

## <sup>1</sup> Sulfonamide Molecular Crystals: Structure, Sublimation <sup>2</sup> Thermodynamic Characteristics, Molecular Packing, Hydrogen Bonds <sup>3</sup> Networks

<sup>4</sup> German L. Perlovich,<sup>\*,†,‡</sup> Alex M. Ryzhakov,<sup>†,‡</sup> Valery V. Tkachev,<sup>‡,§</sup> Lars Kr. Hansen,<sup>||</sup>  
<sup>5</sup> and Oleg A. Raevsky<sup>‡</sup>

<sup>6</sup> <sup>†</sup>Krestov's Institute of Solution Chemistry, Russian Academy of Sciences, 153045 Ivanovo, Russia

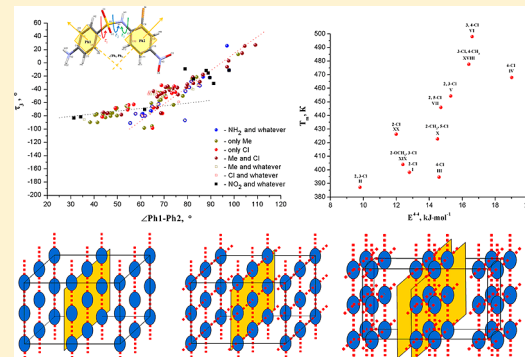
<sup>7</sup> <sup>‡</sup>Institute of Physiologically Active Compounds, Russian Academy of Sciences, 142432 Chernogolovka, Russia

<sup>8</sup> <sup>§</sup>Laboratory of Structural Chemistry, Institute of Problems of Chemical Physics, Russian Academy of Sciences, 142432 Chernogolovka, Russia

<sup>10</sup> <sup>||</sup>Institute of Chemistry, University of Tromsø, Breivika, N-9037 Tromsø, Norway

### 11 Supporting Information

**ABSTRACT:** The crystal structures of ten sulfonamides have been determined by X-ray diffraction. On the basis of our previous data, the obtained results and literature data crystal properties including molecular conformational states, packing architecture, and hydrogen bond networks were comparatively analyzed using graph set notations. Conformational flexibility of the bridge connecting two phenyl rings was studied. It was found out that the most frequently occurring graphs for compounds with a single hydrogen bond are infinite chains with four atoms included. The molecular packing architecture of the selected crystals may be conditionally divided into three different groups. The idea underlying such classification is the difference in structure and composition of molecular layers that can be singled out for most packings. The influence of various molecular fragments on crystal lattice energy was analyzed. A correlation between melting points and fragmental molecular interactions in the crystal lattices was obtained. The thermodynamic aspects of the sulfonamide sublimation were studied by determining the temperature dependence of vapor pressure using the transpiration method. A correlation between the Gibbs energy of the sublimation process and the melting points was found. Besides, a regression equation was derived to describe the correlation between the sublimation entropy terms and crystal density data calculated from X-ray diffraction results.



### 30 ■ INTRODUCTION

Sulfonamides (SA) are an important class of therapeutic agents in modern medical science.<sup>1</sup> The discovery of the first antibiotic "prontosil" was followed by numerous structural modifications of the sulfonylamine molecule to obtain preparations possessing greater antibacterial activity and other pharmacological effects. As a result, compounds possessing anticarbonic anhydrase, antibacterial, diuretic, hypoglycemic, and antihypertensive properties have been produced.<sup>2–4</sup> In addition, most of the recently generated SA derivatives demonstrated antitumor or antiviral activity in vitro and in vivo.<sup>3</sup> Some of the sulfonamide derivatives selected by careful preclinical screening are approved preparations currently under clinical testing.<sup>5</sup>

The increase in the number of new SA derivatives made it necessary to synthesize the compounds involved more rationally and to study their structure/property relationships. As a result, there appeared a number of QSAR publications devoted to both searching for suitable models<sup>6–9</sup> and studying their specific biological activity.<sup>10–12</sup> Such investigations

showed that the biological activity of the sulfonamides depends upon the conformational state of a molecule.<sup>13,14</sup> Due to this fact, it is of primary importance for researchers to study the conformational preferences of compounds containing SA groups as well as to assess the differences in energy content of low-energy conformers.

The constantly growing database on crystalline structures allows the most frequently occurring conformation of sulfonamide molecules in crystals and the difference in conformer energy content to be evaluated. Analysis of conformational states was highlighted in works of Parkin et al.<sup>15</sup> and Brameld et al.<sup>16</sup> The results obtained corroborate the observations of Bock et al.<sup>17</sup> that sulfonamides rarely crystallize in their calculated low-energy structure.

**Received:** May 10, 2013

**Revised:** July 13, 2013

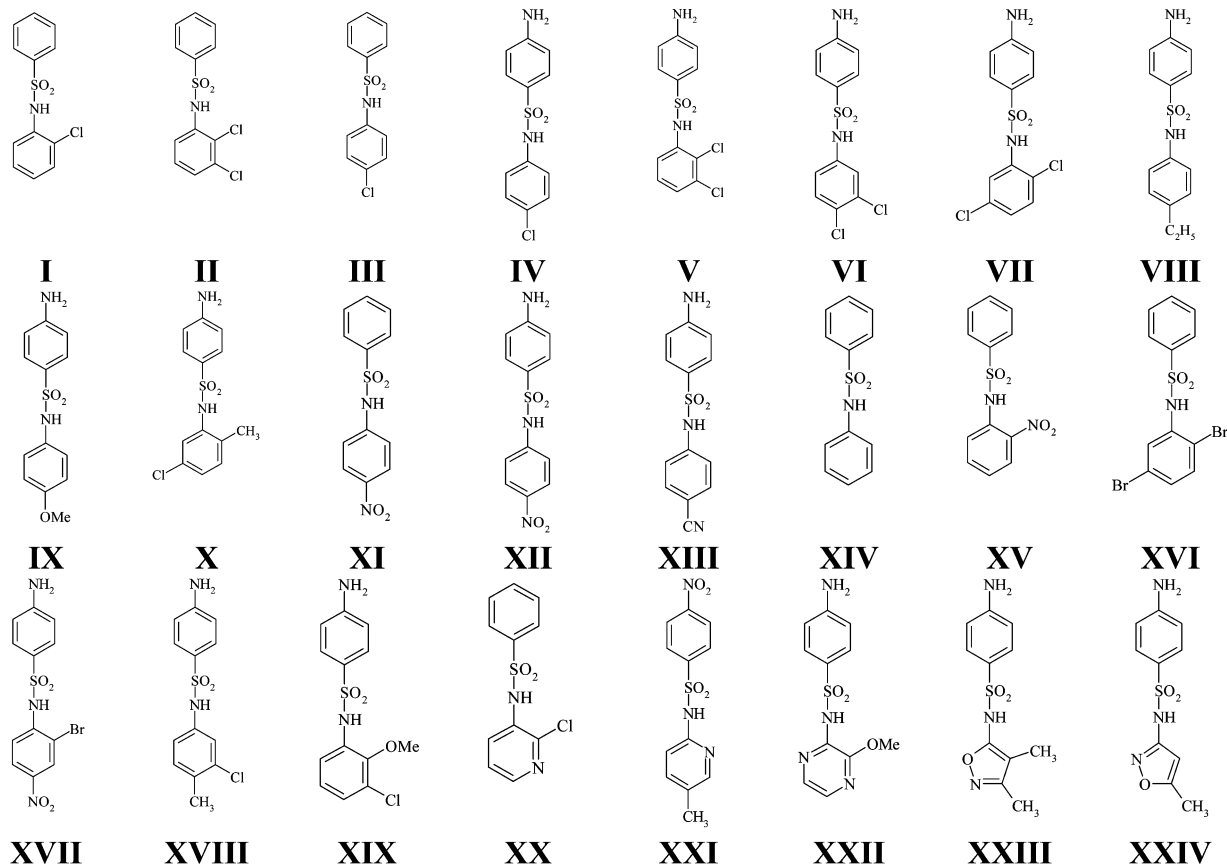


**Figure 1.** Structural formulas of studied substances.

63 Due to the presence of donor and acceptor atoms,  
 64 sulfonamide molecules in a crystal participate in the formation  
 65 of branched hydrogen bond networks. Owing to this fact, the  
 66 compounds concerned are able to form various polymorphic  
 67 forms,<sup>18,19</sup> as well as to become components of various  
 68 complexes<sup>20–22</sup> of cocrystals,<sup>23–25</sup> crystallosolvates,<sup>26–28</sup> and  
 69 even self-assembled organic tubular structures.<sup>29</sup> Thus, the  
 70 studies of sulfonamides are of great interest not only in terms of  
 71 using them as advanced drug compounds but also in terms of  
 72 their crystalline structure as well.

73 Our previous works<sup>30–34</sup> studied the structures, packing  
 74 architecture, topology of hydrogen bond networks, sublimation,  
 75 solubility, and solvation characteristics of 14 sulfonamides (I–  
 76 XIV). As a continuation of the study, this work focuses on the  
 77 comparative analysis of the published compounds with new  
 78 ones: *N*-(2-nitrophenyl)-benzene-sulfonamide (XV), *N*-(2,5-  
 79 dibromophenyl)-benzene-sulfonamide (XVI), 4-amino-*N*-(2-  
 80 bromo-4-nitrophenyl)-benzene-sulfonamide (XVII), 4-amino-  
 81 *N*-(3-chloro-4-methylphenyl)-benzene-sulfonamide (XVIII), 4-  
 82 amino-*N*-(2-methoxy-3-chlorophenyl)-benzene-sulfonamide  
 83 (XIX), *N*-(2-chloro-3-pyridinyl)-benzene-sulfonamide (XX), 4-  
 84 nitro-*N*-(5-methyl-2-pyridinyl)-benzene-sulfonamide (XXI), 4-  
 85 amino-*N*-(3-methoxypyrazinyl)-benzene-sulfonamide (XXII),  
 86 4-amino-*N*-(3,4-dimethyl-5-isoxazolyl)-benzene-sulfonamide  
 87 (XXIII), and 4-amino-*N*-(5-methyl-3-isoxazolyl)-benzene-sul-  
 88 fonamide (XXIV) (Figure 1). The choice of the compounds  
 89 was dictated by the following aims. First, we aimed to analyze  
 90 the influence of substituent nature and molecular topology on  
 91 the molecule conformational state, the formation of crystal  
 92 lattice architecture, and hydrogen bond networks. Second, we  
 93 planned to study the thermodynamic and thermophysical

94 properties of the crystals and find out the relationship between  
 95 the noted parameters and the crystal structure.

## ■ EXPERIMENTAL SECTION

**Compounds and Solvents.** The chemical syntheses of SAs (XV–  
 97 XXIV) have been performed according to the procedures described  
 98 earlier<sup>30–32</sup> by the reaction of a substituted aromatic amine with 4-  
 99 acetylaminobenzenesulfonyl chloride in dry pyridine, followed by  
 100 hydrolytic deacetylation in alkaline aqueous medium (~1 M NaOH),  
 101 and precipitation of the end product by acidification (~1 M HCl) to  
 102 pH 5. The compounds were carefully purified by recrystallizing from a  
 103 water–ethanol solution. The precipitates were filtered and dried at  
 104 room temperature under vacuum until the masses of the compounds  
 105 remained constant. The outlined procedure was repeated several times  
 106 and the product checked by NMR after each recrystallization step until  
 107 the proton NMR signal correspondence to the purity of the compound  
 108 was over 99%. *N*-phenyl-benzene-sulfonamide was obtained from  
 109 Sigma Chemical Co. (USA).

110 Single crystals of the title compounds were grown from a water–  
 111 ethanol solution (initial composition 20:1 v/v) by the vapor diffusion  
 112 of ethanol vapor into pure water.<sup>35</sup>

**Methods.** *X-ray Diffraction Experiments.* Single-crystal X-ray  
 114 measurements were carried out using a Nonius CAD-4 diffractometer  
 115 with graphite monochromated Mo K $\alpha$  radiation ( $\lambda = 0.71069 \text{ \AA}$ ).  
 116 Intensity data were collected at 25 °C by means of a  $\omega$ -2 $\theta$  scanning  
 117 procedure. The crystal structures were solved using direct methods  
 118 and refined by means of a full-matrix least-squares procedure. CAD-4<sup>36</sup>  
 119 was applied for data collection, data reduction, and cell refinement.  
 120 SHELXS-97 and SHELXL-97<sup>37</sup> were used to solve and to refine  
 121 structures, respectively.

*Sublimation Experiments.* Sublimation experiments were carried  
 123 out by the transpiration method as was described elsewhere.<sup>38</sup> In brief,  
 124 a stream of an inert gas passes above the sample at a constant  
 125 temperature and at a known slow constant flow rate in order to  
 126

Table 1. Crystal Lattice Parameters of the Substances under Investigation

	XV <sup>a</sup>	XVI	XVII	XVIII	XIX
CCDC code	930468	930473	930476	930474	930475
crystal system	triclinic	triclinic	monoclinic	orthorhombic	orthorhombic
space group	P $\bar{1}$	P $\bar{1}$	P $2_1/c$	Pna $2_1$	P $2_12_12_1$
crystal size (mm)	0.55 × 0.20 × 0.10	0.50 × 0.35 × 0.20	0.33 × 0.25 × 0.21	0.30 × 0.30 × 0.28	0.30 × 0.20 × 0.10
<i>a</i> (Å)	8.018(2) <sup>b</sup>	8.068(2)	14.740(4)	15.387(3)	7.599(2)
<i>b</i> (Å)	8.569(3)	5.514(1)	5.845(3)	6.273(1)	13.661 (3)
<i>c</i> (Å)	9.992(3)	10.573(2)	16.093(5)	27.363(6)	27.583(6)
$\alpha$ (deg)	86.05(2)	78.51(1)	90.00	90.00	90.00
$\beta$ (deg)	67.05(1)	83.59(1)	92.37(2)	90.00	90.00
$\gamma$ (deg)	77.79(2)	71.11(1)	90.00	90.00	90.00
volume (Å <sup>3</sup> )	617.8(3)	672.6(2)	1385.3(9)	2641.3(9)	2863.4(9)
<i>Z</i>	2	2	4	8	8
<i>D</i> <sub>calc</sub> (g cm <sup>-3</sup> )	1.496	1.931	1.785	1.493	1.451
radiation	Mo K $\alpha$				
<i>T</i> (K)	293	293	293(2)	293(2)	293.1
$\mu$ (mm <sup>-1</sup> )	0.27	6.19	3.137	0.446	0.420
Data Collection					
measured reflections	6121	6542	2692	2669	27680
independend reflections	3162	3458	2588	2669	7779
independend reflections with $>2\sigma(I)$	2182	1533	1689	2391	3252
<i>R</i> <sub>int</sub>	0.021	0.037	0.0525	0.000	0.051
$\theta_{\max}$ (deg)	30.5	30.5	25.57	26.1	30.6
Refinement					
refinement on	<i>F</i> <sup>2</sup>				
<i>R</i> [ <i>F</i> <sup>2</sup> > 2 $\sigma$ ( <i>F</i> <sup>2</sup> )]	0.048	0.036	0.0356	0.0386	0.0546
$\omega R(F^2)$	0.059	0.046	0.0894	0.1022	0.0615
<i>S</i>	0.99	1.05	0.962	1.103	1.127
reflections	2204	1548	2588	2669	3313
parameters	212	172	203	343	387
( $\Delta/\sigma$ ) <sub>max</sub>	0.019	0.021	0.000	0.002	6.546
$\Delta\rho_{\max}$ (e Å <sup>-3</sup> )	0.16	0.64	0.620	0.49	0.49
$\Delta\rho_{\min}$ (e Å <sup>-3</sup> )	-0.28	-0.35	-0.548	-0.26	-0.73
<i>V</i> <sup>dw</sup> (Å <sup>3</sup> )	211.7	237.5	242.2	234.4	244.0
<i>V</i> <sup>free</sup> (Å <sup>3</sup> )	97.2	98.8	104.1	95.8	114.0
$\beta = V^{\text{free}}/V^{\text{dw}}$ (%)	45.9	41.6	43.0	40.9	46.7
K = <i>V</i> <sup>dw</sup> / <i>V</i> <sub>mol</sub> (%)	68.5	70.6	69.9	71.0	68.2
	XX	XXI	XXII <sup>c</sup>	XXIII <sup>d</sup>	XXIV <sup>e</sup>
CCDC code	930467	930469	930470	930471	930472
crystal system	monoclinic	triclinic	orthorhombic	orthorhombic	monoclinic
space group	P $2_1/n$	P $\bar{1}$	P $bca$	P $bca$	C $2/c$
crystal size (mm)	0.57 × 0.49 × 0.41	0.30 × 0.28 × 0.26	0.40 × 0.36 × 0.29	0.45 × 0.40 × 0.32	0.50 × 0.30 × 0.15
<i>a</i> (Å)	10.504(2)	10.408(1)	10.912(1)	14.455(3)	16.079(6)
<i>b</i> (Å)	10.184(2)	11.773(1)	9.514(3)	11.514(2)	5.481 (2)
<i>c</i> (Å)	10.638(2)	12.019(2)	24.842(3)	14.857(3)	25.763(9)
$\alpha$ (deg)	90.00	73.41(1)	90.00	90.00	90.00
$\beta$ (deg)	90.41(2)	69.53(1)	90.00	90.00	96.12(2)
$\gamma$ (deg)	90.00	71.55(1)	90.00	90.00	90.00
volume (Å <sup>3</sup> )	1132.9(4)	1283.2(3)	2598.5(9)	2472.7(9)	2257.4(9)
<i>Z</i>	4	4	8	8	8
<i>D</i> <sub>calc</sub> (g cm <sup>-3</sup> )	1.575	1.518	1.433	1.441	1.490
radiation	Mo K $\alpha$				
<i>T</i> (K)	293(2)	293(2)	293(2)	293(2)	293.1
$\mu$ (mm <sup>-1</sup> )	0.511	0.270	0.259	0.226	0.143
Data Collection					
measured reflections	2329	5291	2708	2605	6333
independend reflections	2211	4480	2066	2450	2875
independend reflections with $>2\sigma(I)$	1839	3660	1372	1737	2009
<i>R</i> <sub>int</sub>	0.019	0.017	0.027	0.081	0.025
$\theta_{\max}$ (deg)	26.00	25.0	25.0	26.1	30.6

Table 1. continued

	XX	XXI	XXII <sup>c</sup>	XXIII <sup>d</sup>	XXIV <sup>e</sup>
	Refinement				
refinement on	$F^2$	$F^2$	$F^2$	$F^2$	$F^2$
$R[F^2 > 2\sigma(F^2)]$	0.0343	0.0396	0.0378	0.0442	0.0435
$\omega R(F^2)$	0.0950	0.1103	0.1114	0.1439	0.0496
$S$	1.046	1.020	1.027	1.110	1.057
reflections	2211	4480	2066	2450	2032
parameters	158	371	194	167	198
$(\Delta/\sigma)_{\text{max}}$	0.001	0.001	0.001	0.001	0.004
$\Delta\rho_{\text{max}} (\text{e } \text{\AA}^{-3})$	0.211	0.37	0.22	0.28	0.32
$\Delta\rho_{\text{min}} (\text{e } \text{\AA}^{-3})$	-0.384	-0.28	-0.29	-0.32	-0.27
$V^{\text{vdw}} (\text{\AA}^3)$	202.4	221.1	220.5	210.5	197.7
$V^{\text{free}} (\text{\AA}^3)$	80.8	99.7	104.3	98.6	84.5
$\beta = V^{\text{free}}/V^{\text{vdw}} (\%)$	40.0	45.1	47.3	46.8	42.7
$K = V^{\text{vdw}}/V_{\text{mol}} (\%)$	71.5	68.9	67.9	68.1	70.1

<sup>a</sup>Ref 64. <sup>b</sup>Standard deviations are presented in brackets. <sup>c</sup>Ref 65. <sup>d</sup>Ref 66. <sup>e</sup>Ref 67.

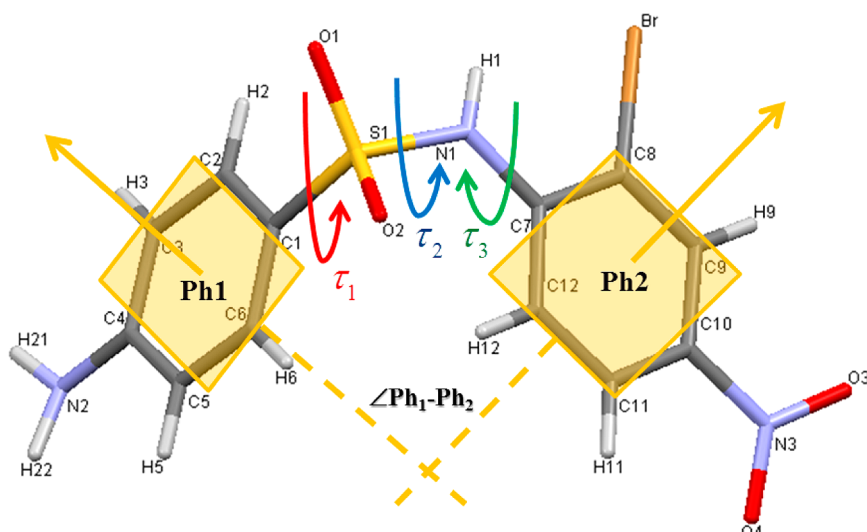


Figure 2. A view of molecule XVII with numbering of atoms and considered angles.

achieve saturation of the carrier gas with the vapor of the substance under investigation. The vapor is condensed at some point downstream, and the mass of sublimate and its purity are determined. The vapor pressure over the sample at this temperature can be calculated by the amount of the sublimated sample and the volume of the inert gas used.

The equipment was calibrated using benzoic acid. The standard value of sublimation enthalpy obtained here was  $\Delta H_{\text{sub}}^0 = 90.5 \pm 0.3 \text{ kJ mol}^{-1}$ . This is in good agreement with the value recommended by IUPAC of  $\Delta H_{\text{sub}}^0 = 89.7 \pm 0.5 \text{ kJ mol}^{-1}$ .<sup>39</sup> The saturated vapor pressures were measured 5 times at each temperature with the standard deviation being within 3–5%. Because the saturated vapor pressure of the investigated compounds is low, it may be assumed that the heat capacity change of the vapor with temperature is so small that it can be neglected. The experimentally determined vapor pressure data may be described in  $(\ln P; 1/T)$  coordinates in the following way:

$$\ln(P) = A + B/T \quad (1)$$

The value of the sublimation enthalpy is calculated by the Clausius–Clapeyron equation:

$$\Delta H_{\text{sub}}^T = RT^2 \partial(\ln P) / \partial(T) \quad (2)$$

whereas the sublimation entropy at the given temperature ( $T$ ) was calculated from the following relation:

$$\Delta S_{\text{sub}}^T = (\Delta H_{\text{sub}}^T - \Delta G_{\text{sub}}^T) / T \quad (3)$$

with  $\Delta G_{\text{sub}}^T = -RT \ln(P/P_0)$ , where  $P_0$  is the standard pressure of  $1 \times 10^5 \text{ Pa}$ .

For experimental reasons sublimation data are obtained at elevated temperatures. However, in comparison with effusion methods, the temperatures are much lower, which makes extrapolation to room conditions easier. In order to further improve the extrapolation to room conditions, we estimated the heat capacities ( $C_{\text{p,cr}}^{298}$  value) of the crystals using the additive scheme proposed by Chickos et al.<sup>40</sup> Heat capacity was introduced as a correction for the recalculation of the sublimation enthalpy  $\Delta H_{\text{sub}}^T$  value at 298 K ( $\Delta H_{\text{sub}}^{298}$  value), according to the equation:<sup>40</sup>

$$\Delta H_{\text{sub}}^{298} = \Delta H_{\text{sub}}^T + \Delta H_{\text{cor}} = \Delta H_{\text{sub}}^T + (0.75 + 0.15C_{\text{p,cr}}^{298})(T - 298.15) \quad (4)$$

**Differential Scanning Calorimetry.** Differential scanning calorimetry (DSC) was carried out using a Perkin-Elmer Pyris 1 DSC differential scanning calorimeter (Perkin-Elmer Analytical Instruments, Norwalk, Connecticut) with Pyris for Windows NT. DSC runs were performed in an atmosphere of flowing (20 mL min<sup>-1</sup>) dry helium gas of high purity 99.996%, using standard aluminum sample pans and a heating rate of 10 K min<sup>-1</sup>. The accuracy of weight measurements was  $\pm 0.005 \text{ mg}$ . The DSC was calibrated with an indium sample from Perkin-Elmer (P/N 0319-0033). The value determined for the enthalpy of fusion corresponded to 28.48 J g<sup>-1</sup> [reference value

172 28.45 J g<sup>-1</sup>]. The melting point was 156.5 ± 0.1 °C (*n* = 10). The  
173 enthalpy of fusion at 298 K was calculated by the following equation:

174  $\Delta H_{\text{fus}}^{298} = \Delta H_{\text{fus}}^T - \Delta S_{\text{fus}}^T(T_m - 298.15)$  (5)

175 where the difference between the heat capacities of the melt and solid  
176 states was approximated by the fusion entropy (as an upper estimate).  
177 This approach was used by Dannenfelsler and Yalkowsky.<sup>41</sup>

178 **Calculation Procedure.** The free molecular volume in the crystal  
179 lattice was estimated on the basis of the X-ray diffraction data and van  
180 der Waals molecular volume ( $V^{\text{vdw}}$ ), calculated by GEOPOL<sup>42</sup>

181  $V^{\text{free}} = (V_{\text{cell}} - ZV^{\text{vdw}})/Z$  (6)

182 where  $V_{\text{cell}}$  is the volume of the unit cell and  $Z$  is the number of  
183 molecules in the unit cell.

184 Nonbonded van der Waals interactions of crystal lattice energy were  
185 calculated as a sum of atom–atom interactions with the help of a  
186 Gavezzotti et al.<sup>43</sup> force field and cutoff radius of 16 Å.

187 The torsion angle stress energies ( $E_{\text{tor}}$ ) were obtained from the  
188 software environment “Accelrys Materials Studio”, using the Forceit  
189 classical molecular mechanics code as a model engine.<sup>48</sup>

## 190 ■ RESULTS AND DISCUSSION

191 **Crystal Structure Analysis.** The results of X-ray diffraction  
192 experiments are presented in Table 1.

193 Though most of the sulfonamides exist as amide tautomers,  
194 there are some well-known exceptions. Imide tautomers for  
195 crystals of sulfanylamide,<sup>44</sup> sulfamethoxydiazine,<sup>45</sup> sulfadox-  
196 ine,<sup>46</sup> sulfisoxazole,<sup>46</sup> sulfothiazole,<sup>47,48</sup> and sulfaguanidine<sup>49</sup>  
197 have been revealed earlier. Three polymorphic forms of  
198 sulpiride have been described in the works of Bar and  
199 Bernstein,<sup>50</sup> all of them existing in an imide form. Among  
200 crystal structures considered, compound XXI has the form of  
201 an imide tautomer. The compound is a heterocyclic  
202 sulfonamide with a nitrogen atom in the ortho-position in  
203 the second ring. Due to the competitive position of two  
204 nitrogen atoms, the amide proton can migrate into a  
205 heterocyclic ring. However, as one can see from the structures  
206 of XXII and XXIV, the presence of nitrogen in the ortho  
207 position adjacent to an amide group of the ring is not enough  
208 for an imide tautomer to be formed.

209 **Molecular Conformational Analysis.** In order to characterize  
210 the conformational states of the molecules, Figure 2 shows  
211 the view of representative molecule XVII with atomic  
212 numbering. This numbering was used for all the compounds  
213 under investigation. Compounds XIII, XVII, XIX, and XXI  
214 have two molecules (A and B) in the asymmetric unit of the  
215 crystal lattice. On the basis of the presented numbering, it is  
216 possible to carry out the comparative analysis of conformational  
217 states of molecules I–XXIV. The conformational states of the  
218 molecules under investigation depend on the mobility of the  
219 bridge, connecting two phenyl rings. In order to describe the  
220 conformational state, we have chosen three parameters  
221 (analogous to Parkin et al.<sup>15</sup>): the angle between the SO<sub>2</sub>  
222 group and the phenyl motif Ph 1 (C1–C2–C3–C4–C5–C6)  
223  $\angle C_2–C_1–S_1–N_1$  ( $\tau_1$ ), the angle  $\angle C_7–N_1–S_1–C_1$  ( $\tau_2$ ),  
224 describing the S1–N1 bond mobility, and the torsion angle  
225  $\angle C_{12}–C_7–N_1–S_1$  ( $\tau_3$ ), which characterizes the location of  
226 the second phenyl ring Ph2 (C7–C8–C9–C10–C11–C12)  
227 relative to the NH group. Moreover, we introduced an angle  
228 between the two phenyl rings  $\angle \text{Ph1–Ph2}$  (the acute angle  
229 between the least-squares planes through the two phenyl rings)  
230 (Table 1 of the Supporting Information). In addition to the  
231 noted angles we introduced an angle, equal to the sum of the  
232 dihedral angles ( $\sum \tau_i = \tau_1 + \tau_2 + \tau_3$ ), which describes the

233 integral flexibility of the bridge connecting the phenyl rings. As  
234 it has been demonstrated in our previous work<sup>34</sup> (using a limited  
235 number of sulfonamides), there is a correlation between  $\tau_3$  and  $\angle \text{Ph1–Ph2}$ . To confirm the discovered regularities, we extended  
236 the range of SA, investigated by including the structures presented in the literature (ref codes are given in Table 2 of the Supporting Information), and analyzed their conformational states. The results of the analysis are shown in Figure 3. All the compounds are divided into groups,

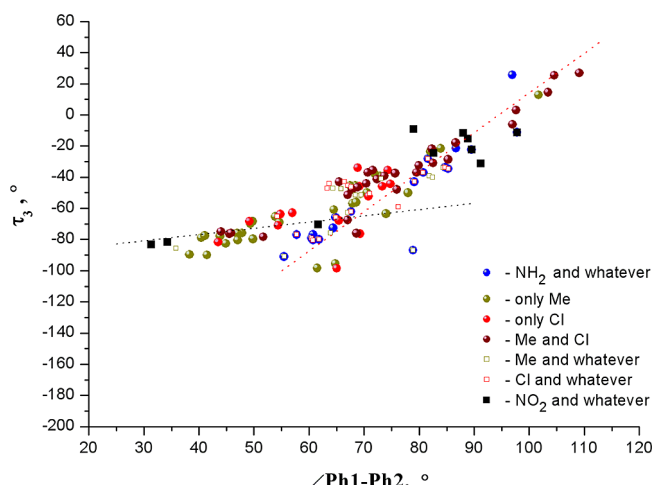


Figure 3. Plot of  $\tau_3$  vs  $\angle \text{Ph1–Ph2}$  (see Figure 2) for the compounds studied in this work and literature data (color corresponds to the different groups of SA; see the text).

242 depending on the substituents available in phenyl rings. Some  
243 points lay over each other, which indicates the presence of several  
244 substituents in phenyl fragments.  $\tau_3$  and  $\angle \text{Ph1–Ph2}$  are well-correlated. So, angle  $\tau_3$ , making a major contribution in the turn between two phenyl rings, is most susceptible to structural changes of SA molecules. We would like to emphasize that all experimental data are subdivided into a low-angle branch [according to the  $\angle \text{Ph1–Ph2}$  angle (black dotted line)] and a high-angle one (red dotted line). A slight change in  $\tau_3$  for the low-angle branch results in a considerable change of the angle between the phenyl rings. This change is far less pronounced for the high-angle branch. Some of the investigated compounds possess two molecules in asymmetric units. In view of this fact, we attempted to analyze the ways in which such SAs are distributed in the branches involved. It was found out that most of the compounds with two molecules in the asymmetric unit belong to the high-angle branch. Then, we determined the percentage of these compounds within the limits of groups/clusters, into which all SA compounds have been subdivided (see Figure 3). It was found out that 54% of SA with NH<sub>2</sub>– and any other group as substituents in phenyl rings are compounds with two molecules. The results obtained for other compounds are as follows: Cl– and any other group, –36%; Me– and any other group, –18%; NO<sub>2</sub>– and any other group, –11%; Cl– and Me–, 17%; only Me–, 19%; and only Cl–, 8%. Thus, SAs with an amine group are distinguished by a maximum number of compounds with two molecules in an asymmetric unit; it follows from the increased number of hydrogen bonds per molecule (as compared to compounds with other groups) and the presence of molecular networks with a complex topological structure (see below). One can assume that it is the compounds

273 with the amine group that show a greater tendency to form  
274 polymorphic forms as compared to the others we considered.

275 Our next step was to study SA with two molecules in the  
276 asymmetric unit. Comparative analysis of the torsion angle  
277 stress energy of molecules A and B was carried out. Conformer  
278 A (being a high-angle one) appeared to be more relaxed (that  
279 is, it had less torsion stress energy,  $E_{\text{tor}}$ ) in comparison with  
280 conformer B. If we take the difference in angles between phenyl  
281 fragments of conformers A and B as a standard distinction  
282 between them, we will see that their values vary over a wide  
283 range: from  $1^\circ$  to  $47^\circ$ . Figure 4 presents these values as a

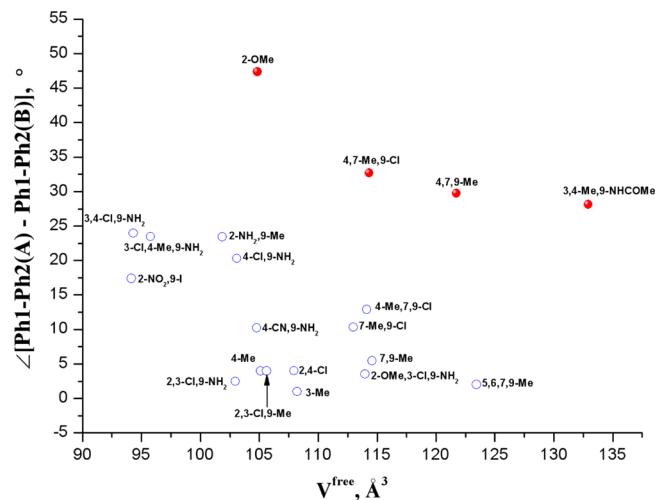
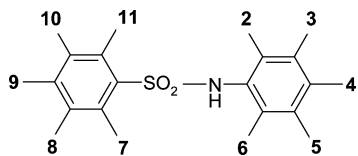


Figure 4. Plot of angles difference between the phenyl rings of the conformers A and B versus the free volume per molecule in the crystal (numbering substituents corresponds to Scheme 1).

284 function of free volume values per molecule (the numbering of  
285 a substituent position in SA molecule corresponds to that in  
286 Scheme 1). As one can see, all dots may be arbitrarily

### Scheme 1



287 subdivided into two groups: the first one has a greater spread in  
288 angle values between the conformers (red ●), while the second  
289 one has a smaller spread in contrast to the first one (blue ○).  
290 The regularities in changes of the values discussed are as  
291 follows: the free volume per molecule in a crystal occurs the  
292 most; the difference in the angles between phenyl fragments of  
293 the conformers occurs the least. Unfortunately, we failed to  
294 identify any regularities between the structures of the  
295 compounds of both groups. The only thing we can emphasize  
296 is that the compounds containing amino substituents (with an  
297 added number of hydrogen bonds per molecule) are in the  
298 second group.

299 As it has already been emphasized, the literature contains  
300 many experimental data describing crystal structure of methyl  
301 and chlorine derivatives of SA. We adopted these data to make  
302 it easier to study how the number, the position, and the nature  
303 of substituents affect the density of molecular packing in a  
304 crystal. Experimental values of the compounds involved were

305 plotted as  $\beta = V^{\text{free}}/V^{\text{vdw}}$  versus  $V^{\text{vdw}}$  and  $V^{\text{free}}$  versus  $V^{\text{vdw}}$   
306 (Figures 1, 2, and 3 of the Supporting Information). Figure 5  
307

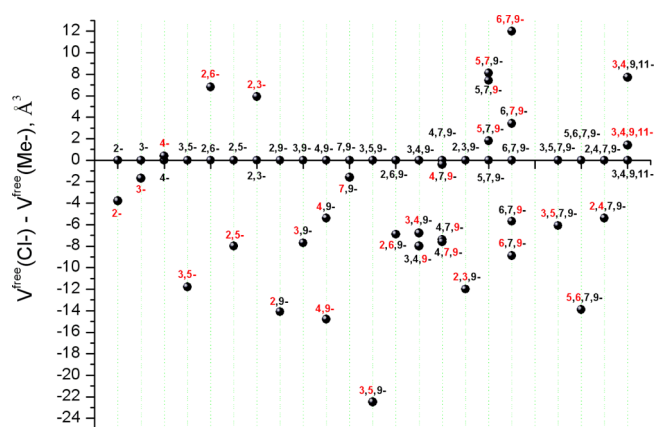
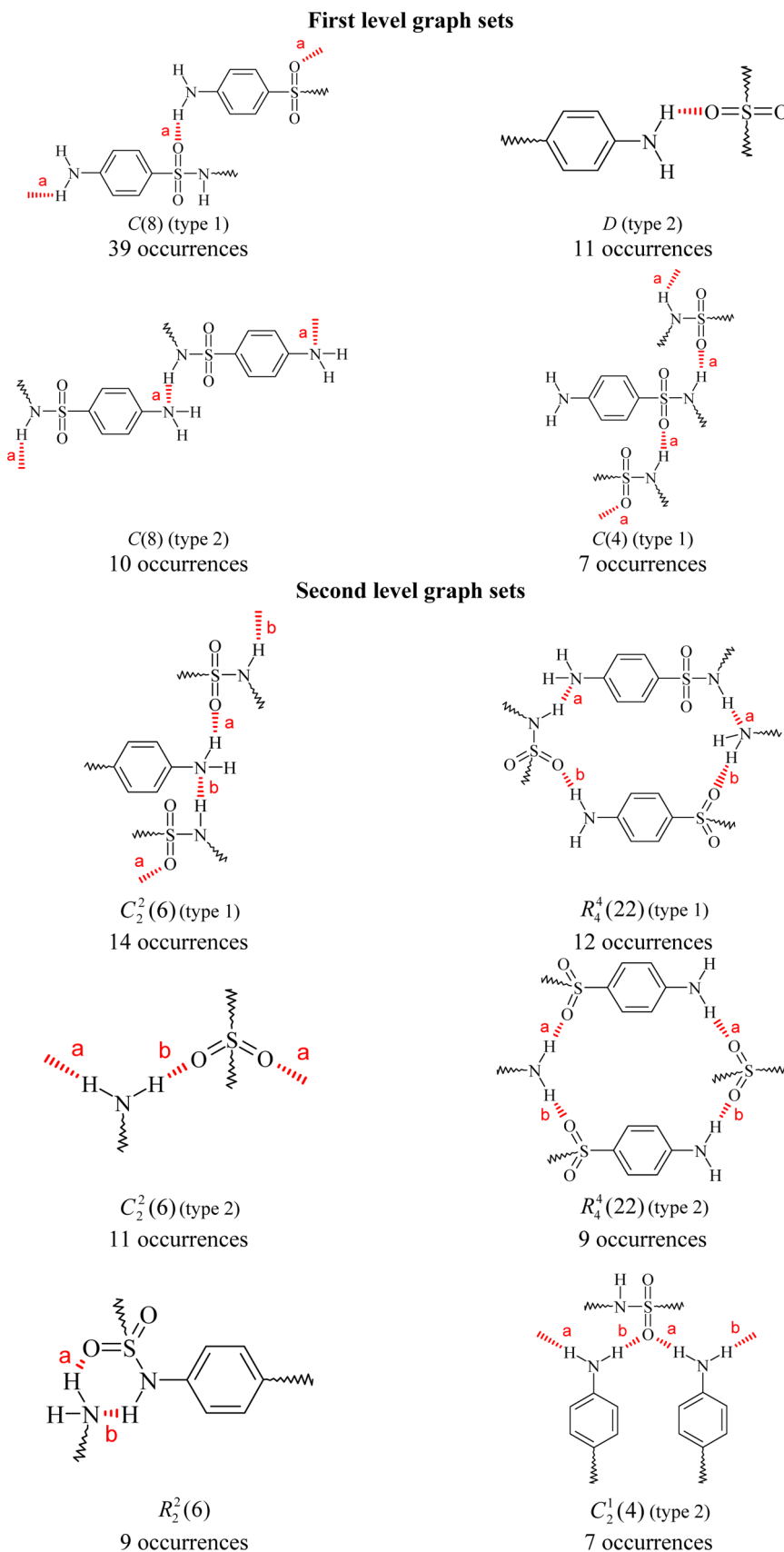


Figure 5. Plot of free volumes difference of SA studied at the replacement locations of Me- on Cl- groups located at the same positions (red corresponds to Cl- atoms, black to Me-). Numbering corresponds to Scheme 1.

308 presents the results of changing the free volume of SA with  
309 Me- substituted by Cl- groups in similar positions (Cl-  
310 atoms are marked by red, Me- groups by black). The  
311 numbering of the positions corresponds to that in Scheme 1.  
312

313 For monosubstituted derivatives, replacement of methyl  
314 groups by chlorine is accompanied by a reduction in the free  
315 volume, the exception being the para position (a slight  
316 increase). For disubstituted SA, substitution of two Me-  
317 atoms by Cl- results in both a decrease in free volumes (3,5-;  
318 2,5-; and 4,9-) and their adding (2,6- and 2,3-). Substitution of  
319 a Me- group for Cl- in 2-, 3-, 4-, and 7- positions of the  
320 dimerivative of SA (the second Me- remaining invariably in the  
321 9-position) causes the free volume to decrease. The pattern for  
322 free-derivatives of SA becomes more complicated. If one of the  
323 substituents is in position 9- in the first phenyl fragment, while  
324 the two others are in the second fragment (3,5,9-; 2,6,9-; 3,4,9-;  
325 and 2,3,9-), only a decrease in the free volume takes place. If  
326 two substituents are in positions 7- and 9- in the first phenyl  
327 fragment, while the others remain in the second phenyl ring  
328 (4,7,9-; 5,7,9-; and 6,7,9-), the free volume only diminishes for  
329 4,7,9-, while for 6,7,9-, it either increases or decreases. The  
330 substitution of all methyl groups for Cl- causes a significant  
331 free volume increase for 6,7,9-. The pattern for tetrasubstituted  
332 SA cannot be regarded as a simple one. The substitution  
333 reduces the free volume for three compounds (3,5,7,9-; 5,6,7,9-;  
334 and 2,4,7,9-) and increases it for 3,4,9,11-. The substitution of  
335 the four methyl groups by Cl- atoms in 3,4,9,11- gives a  
336 negligible change in free volume.

337 *Hydrogen Bond Network Analysis.* The compounds  
338 considered are able to form hydrogen bonds in crystal lattices.  
339 Moreover, the number of hydrogen bonds in a molecule varies  
340 remarkably and depends on the topology of a molecule and the  
341 presence of hydrogen bond centers. Hydrogen bonds form  
342 chains with various topological structures, which influences  
343 thermodynamic and thermophysical characteristics, crystal  
344 lattice energy, and as a consequence, the processes of  
345 dissolution. The next block of our investigations consisted in  
346 analysis of the hydrogen bond network topology, using the  
347 terms of topological graphs introduced by Etter<sup>51</sup> and  
348 supplemented by Bernstein.<sup>52</sup> Table 3 of the Supporting  
349



**Figure 6.** Distribution of frequently observed hydrogen-bond motifs of first and second levels (schematic, graph set, and number of occurrences).

347 Information shows the results of comparative analysis of  
348 hydrogen bond geometrical parameters, as well as the matrix of

349 topological graphs describing the network topology of the 349  
molecular crystals under study for the first (diagonal elements) 350

351 and the second (subdiagonal elements) levels. All the  
 352 topological graphs occurring in crystals are given schematically  
 353 in Table 4 of the Supporting Information. The crystal structures  
 354 of all the compounds investigated contain 16 various graphs of  
 355 the first level (with only one type of hydrogen bond  
 356 participating) and 35 graphs of the second level (with hydrogen  
 357 bonds of two types participating). The most prevalent  
 358 hydrogen-bond motifs for both levels are given in Figure 6.

359 The simplest hydrogen bond network is observed for  
 360 compounds I, II, III, XI, XIV, XV, XVI, and XX, as only one  
 361 hydrogen bond participates in their formation. It is caused by  
 362 the fact that it is the sulfonamide group with an amide proton  
 363 as a bond donor that becomes the only center of the hydrogen  
 364 bond. The presence of additional acceptor groups (as for XI,  
 365 XV, and XX) does not account for the growth of hydrogen  
 366 bonds. Figure 7 shows the histograms of the most frequently

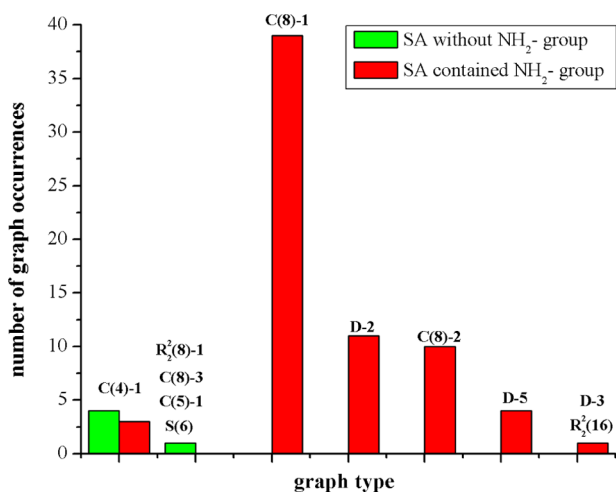


Figure 7. Frequency of occurrence of different topological graphs of the first level at the presence and absence of the amino-group at the first phenyl ring of SA studied (designations of the graphs correspond to Table 4 of the Supporting Information).

367 occurring graphs of the compounds with (a) a single hydrogen  
 368 bond (sulfonamides without an amide group in the first phenyl  
 369 ring, green) and (b) an amino group (with several hydrogen  
 370 bonds, red). As one can see from Figure 6, the most frequently  
 371 occurring graphs for the compounds with a single hydrogen  
 372 bond are infinite chains with four included atoms C(4)-1.  
 373 Introducing NH<sub>2</sub>- groups (additional centers of hydrogen  
 374 bond formation) into the first phenyl ring makes topological  
 375 graphs change considerably. Only sinton C(4)-1 remains, while  
 376 6 new graphs appear with the most frequently occurring one  
 377 being C(8)-1.

378 Let us consider the way in which network topology changes  
 379 for comparable structures. Thus, for example, the introduction  
 380 of NH<sub>2</sub>- groups into compounds II, III, and XI (as a result, we  
 381 obtain compounds V, IV, and XII, respectively) causes the  
 382 hydrogen bond network to change remarkably. Due to adding a  
 383 new hydrogen bond center into the first phenyl ring, the  
 384 number of hydrogen bonds grows from 1 to 3.5 (7 for two  
 385 molecules in the asymmetric unit) for V, 4 for IV, and 3 for XII.  
 386 Moreover, amine-derivative compounds do not possess hydro-  
 387 gen bonds that are realized in II, III, and XI. As a result, we  
 388 obtain the following change in the topological graphs for  
 389 comparable pairs of compounds in crystals and, as an outcome,  
 390 the topology of their networks. Compound II has a single

391 C(4)-1 graph, while compound V possesses three different 391  
 392 graphs: R<sub>2</sub>(16), D-2, and D-5 (Table 4 of the Supporting 392  
 393 Information). There is only one sinton for compound III C(4)- 393  
 394 1, while there are three graphs for compound IV: C(8)-1, C(8)- 394  
 395 2, and D-2. There is only a C(8)-3 graph available for 395  
 396 compound XI, while two different graphs are available for V: 396  
 397 C(8)-1 and C(8)-2. 397

398 For all the sulfonamides investigated, it is only amido- (N1) 398  
 399 and amino- (N2) protons that are donors of hydrogen bonds. 399  
 400 Proceeding from this fact, we attempted to evaluate the extent 400  
 401 of their participation in the formation of hydrogen bond 401  
 402 networks. The results of the analysis expressed as a percentage 402  
 403 ratio for two different types of donors are shown in Table 2. It 403 t2

Table 2. Hydrogen-Bonding Frequency Observed for Amido and Amino Protons

donor	general number of HBs in structures contained the type of donor	number of HBs formed by this donor type	% of involvement
amido (N1) proton	82	35	42.7
amino (N2) proton	74	52	70.3

404 may be noticed that the amino proton participates about 1.5 404  
 405 times as often as the amido proton in the formation of 405  
 406 hydrogen bond networks. It is most likely to be associated with 406  
 407 the way hydrogen atoms are arranged: being in the outlying 407  
 408 part of a molecule, they are available for the formation of bonds 408  
 409 with adjacent molecules. Amido protons are within the 409  
 410 molecule and are closed down partly by other fragments. The 410  
 411 latter fact becomes a barrier to the process. Analysis of 411  
 412 hydrogen bonds of protodonor groups concerned has showed 412  
 413 that about 51 in 52 cases, the amino group participates in an 413  
 414 -NH<sub>2</sub>...SO<sub>2</sub> bond and in about 9 in 35 cases (25.7%) it forms 414  
 415 an -NH...SO<sub>2</sub> bond. It would be interesting to emphasize 415  
 416 that in the above-mentioned compounds the amino group is 416  
 417 able to act as a hydrogen bond acceptor. The number of these 417  
 418 bonds amounts to 51.9% for the amido proton and corresponds 418  
 419 to C(8)-2 graphs. 419

420 Hydrogen bond networks of the second level (i.e., formed by 420  
 421 different bonds) are combinations of various graphs of the first 421  
 422 level. This combination of graphs is expressed in the form of 422  
 423 unique infinite chains as well as rings with various numbers of 423  
 424 atoms involved. Figure 4 of the Supporting Information shows 424  
 425 the most frequently occurring second level graphs. 425

426 *Packing Architecture Analysis.* The molecular packing 426  
 427 architecture of crystals depends on the molecular structure 427  
 428 and topology. The compounds under consideration are 428  
 429 structurally similar. Therefore, variations of size, nature, and 429  
 430 position of substituents make it possible to analyze the 430  
 431 influence of these factors on the packing architecture. The 431  
 432 molecular packing architectures of the new substances under 432  
 433 investigation are presented in Figure 5 of the Supporting 433  
 434 Information. 434

435 The molecular packing architecture in the crystals of I- 435  
 436 XXIV compounds may be subdivided into three groups. The 436  
 437 division is based on the difference in structure and composition 437  
 438 of molecular layers to be singled out for most of the packing 438  
 439 f8

440 The topology of the first groups is of the same character. 440  
 441 They include compounds I, II, III, VII, X, XI, XIV, XX, XXIII, 441

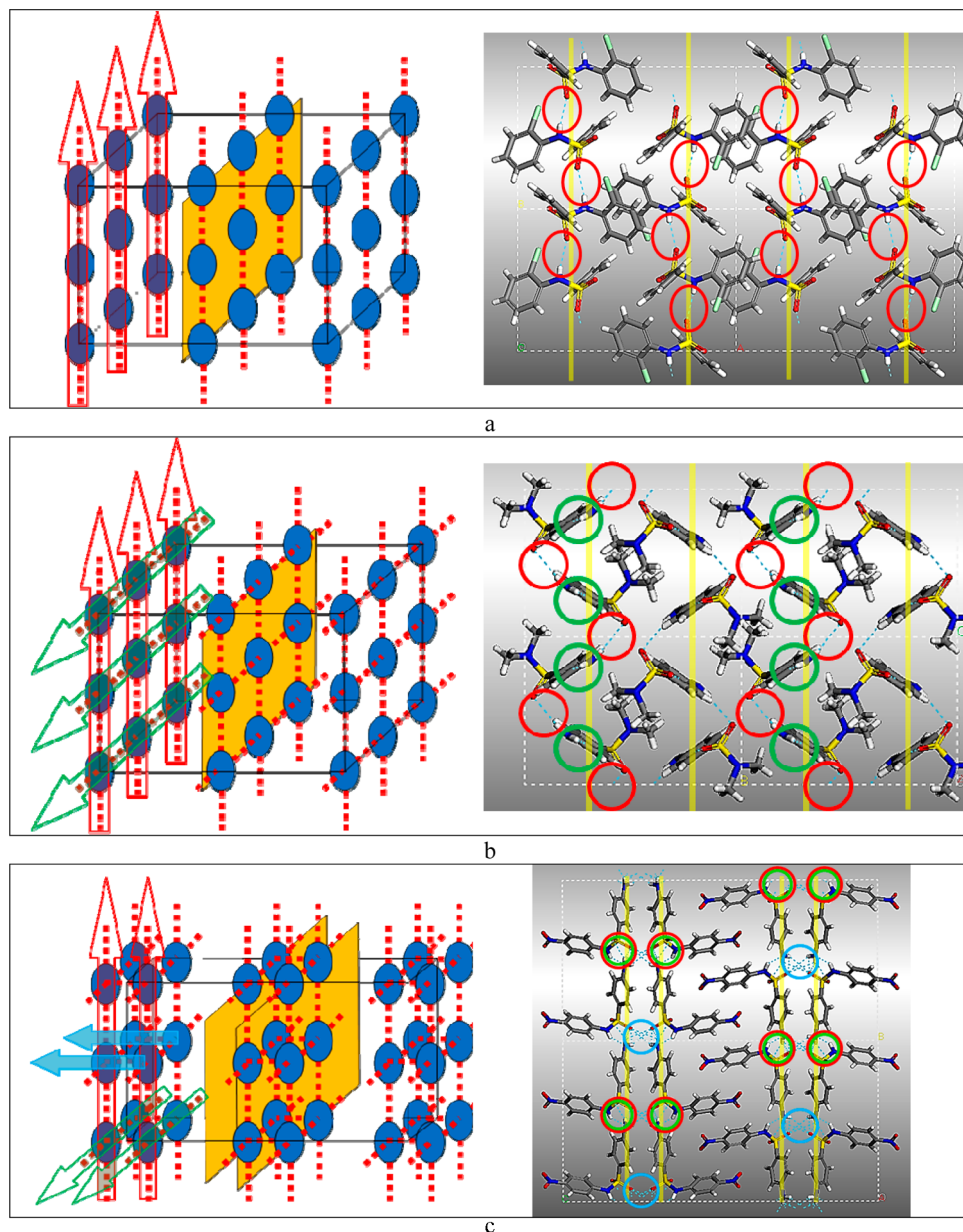


**Figure 8.** A layout view of molecular packing and hydrogen bond networks of SA studied in the crystals [(a) compounds of I, (b) II, and (c) III groups]. Actual examples of the corresponding crystal structures for each group are shown on the right. Hydrogen bond chains with different dimensional orientations are marked by varicolored circles and arrows.

and **XXIV**. The specific feature of the compounds is having equally distant layers formed by infinite chains of hydrogen bonds C(4), C(5), and C(8). The adjacent layers interact by means of van der Waals forces, while the way the molecule chains interact within the layer may vary. For the first group of compounds (**I**, **II**, **III**, **XI**, and **XIV**) bonding is brought about through van der Waals forces (Figure 8a). It would be interesting to note that for most members of this subgroup, the layers have the same direction in relation to the hydrogen bond networks. For the crystals of compound **XIV**, the adjacent layers are turned at the angle of 90° relative to each other. For the second group of compounds (**VII**, **X**, **XXIII**, and **XXIV**), the adjacent molecule chains are linked with a hydrogen bond to form two-dimensional networks (Figure 8b).

The pattern of the compounds of group III is similar to the previous ones. The difference consists in the fact that the

interlayer interactions are realized in turn through a hydrogen bond and van der Waals forces. Thus, this specific group is distinguished by two layers formed by pairs of intertwining (intertangling) chains of molecules. All the molecules inside of the bilayer are linked by hydrogen bonding, while those of various bilayers interact only through van der Waals forces. This group includes compounds **IV**, **V**, **VI**, **VIII**, **IX**, **XII**, **XVII**, **XVIII**, **XIX**, and **XXII**.

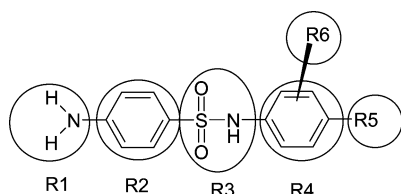
Samples of the compounds investigated have two dimeric structures, **XVI** and **XXI**. Molecules of these crystals are linked in pairs by a hydrogen bond to form graph  $R_2^2(8)$ . It should be noted that the asymmetric crystal unit of **XXI** consists of two molecules, dimers being formed between the molecules of the same conformational state (A–A and B–B). In both compounds, the first and second phenyl rings are in parallel position relative to each other.

The crystals of **XIII** and **XV** have a distinctive character. A three-dimensional network of hydrogen bonds is formed in a crystal lattice of **XIII**, thereby making the architecture of the compound molecule packing dramatically different from the above-mentioned ones, its subdivision into layers is not presumed. Conversely, intermolecular hydrogen bonds are not available in compound **XV**. However, one cannot help but notice their similarity to the compounds of the first group, with the only difference between them consisting in the fact that all interactions between their molecules are influenced by van der Waals forces.

Literature data analysis (see Table 2 of the Supporting Information) has shown that most of the similar structures possess one or two hydrogen bonds of different types. As a result, the molecules of the compounds published are packed in a crystal lattice either in the form of dimers (**2, 6, 8, 12, 15–17, 19–21, 22–44, 50, 51, 53, 54, 56–64, 69–73, 75–77, 80, 84–86, 88, 90–92, 96, 98, 100–102, and 107**) or in the form of infinite chains of the first group of compounds (**1, 13, 14, 18, 45–49, 52, 55, 65, 68, 74, 78, 81, 82, 87, 89, 93–95, 97, 103, 104, and 106**).

In order to understand the influence of various molecular fragments on the crystal lattice energy, we used the approach applied by us earlier.<sup>53</sup> The molecule was conditionally divided into a certain number of fragments, depending on the molecular topology. Segmentation for the six fragments (as a common case) is shown in Scheme 2. After that, we calculated the contribution of nonbonded van der Waals interactions to the packing energy from different fragment pairs of adjacent molecules.

Scheme 2



The results of the contributions made by the calculated fragments to the crystal lattice energy of compounds **XV–XXIV** are presented in Figure 9 in coordinates that characterize the package density of the molecules in a crystal.

While studying the para- and aminoderivatives of sulfonamides with two substituents in the second phenyl ring, we revealed the following regularities (Figure 10). The critical contributions stabilizing crystal lattices are interactions between identical phenyl rings and the first phenyl ring and a bridge. It was interesting to note that as soon as the molecule package density in a crystal reaches a certain value (red dotted line), one observes an inversion in the interaction contributions between the second fragments (2–2) and between the second and the third ones (2–3). The contributions of the interactions between the first phenyl rings (2–2) of adjacent molecules to the crystal lattice of compounds **V, VII, X, and XIX** are drastically different from each other, being only 5 kJ less than comparable (equivalent) values for **VI, XVII, and XVIII**. Thus, for sulfonamides with a denser molecule packing, the critical contributions stabilizing the crystal lattice correspond to the interactions between identical phenyl fragments ( $\text{R}_2-\text{R}_2$  and  $\text{R}_4-\text{R}_4$ ) of adjacent molecules. As for the rest of the

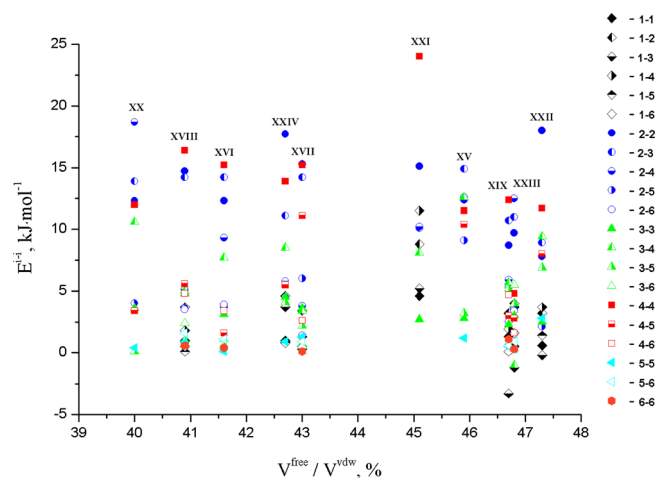


Figure 9. Relationship between the contributions from various molecular fragments in the packing energy made by the nonbonded van der Waals interactions ( $E^{i-i}$ ) and  $V^{\text{free}} / V^{\text{vdw}}$ . Numbering corresponds to Scheme 2.

compounds, it is the bridge connecting two aromatic rings that interferes in the energy distribution:  $\text{R}_4-\text{R}_4$  and  $\text{R}_2-\text{R}_3$ .

Our next step was to compare the crystal packing of different groups of compounds and the main fragment contributions of the compounds involved to the crystal lattice energy stabilization. As a result, it was found out that for the compounds of group I, the main contributions to crystal lattice energy stabilization are the interactions between the first and the second phenyl rings, as well as those between the bridge and the second phenyl fragment of adjacent molecules ( $\text{R}_2-\text{R}_4$  and  $\text{R}_2-\text{R}_3$ ). For the sulfonamides of group II, the main contributions are, in their turn, the interactions between the second phenyl rings, as well as those between the first ring and the bridge ( $\text{R}_4-\text{R}_4$  and  $\text{R}_2-\text{R}_3$ ). It is the interactions between identical phenyl rings of adjacent molecules ( $\text{R}_2-\text{R}_2$  and  $\text{R}_4-\text{R}_4$ ) that are the dominating contributions to the crystal lattice energy of the compounds of group 3.

**Sublimation Characteristics.** The temperature dependences of saturated vapor pressure of **XVI–XXIV** are shown in Table 5 of the Supporting Information. The thermodynamic functions of drug sublimation and fusion processes are presented in Table 3.

The problem constantly occupying the minds of scientists in the literature<sup>54–57</sup> is the determination of regularities in the interrelations between thermodynamic (sublimation) and thermophysical (fusion processes) characteristics and parameters of crystal structures. Long ago, Kitaigorodsky<sup>58</sup> suggested that various physicochemical properties should be correlated with the parameters describing molecule package density in a crystal ( $V^{\text{vdw}}/V^{\text{mol}}$ ). The parameter ( $\beta = V^{\text{free}}/V^{\text{vdw}}$ ) has been slightly modified in some works,<sup>59–61</sup> as the authors wanted to pay special attention to the free volume ( $V^{\text{free}}$ ) per molecule in a crystal. In this context,  $V^{\text{free}}$  is an integral value including: (a) free volume formed as a result of a complex topological structure and steric hindrance from conformationally mobile molecules in a crystal (the so-called “free volume” dependent on molecule structure in a conformational state in a crystal) and (b) free volume formed as a result of the molecular package in a crystal (these being equivalent under given parameters of crystal defects packing). It is difficult to differentiate between the two defects, but their participation in the processes

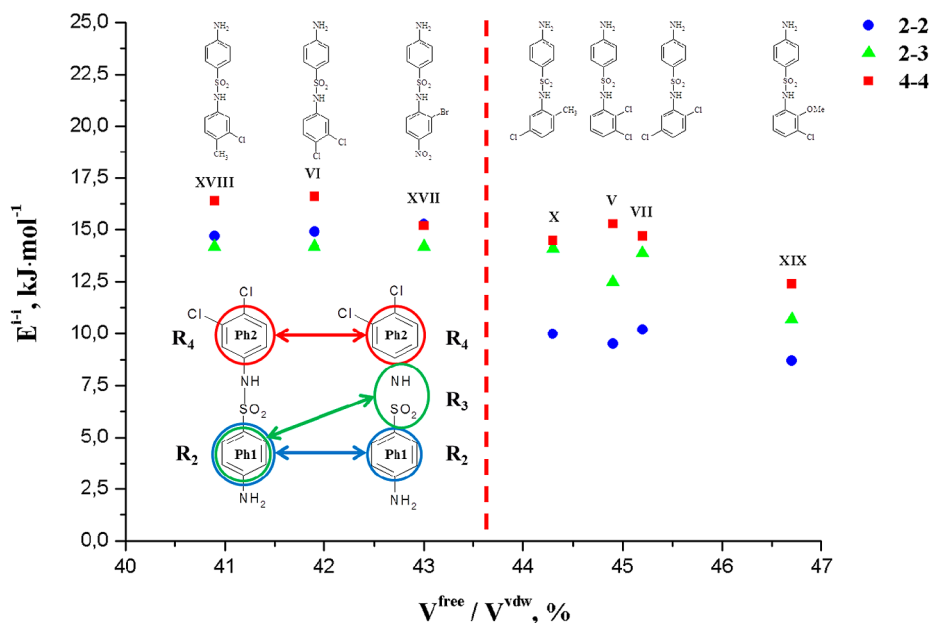


**Figure 10.** Relationship between the contributions from various molecular fragments in the packing energy ( $E^{i-i}$ ) and  $V^{\text{free}}/V^{\text{vdw}}$  for para-, amino-SA with two substituents at the second phenyl ring.

**Table 3. Thermodynamic Characteristics of Sublimation and Fusion Processes of the Compounds Studied**

	XV	XVII	XVIII	XIX	XXII
$\Delta G_{\text{sub}}^{298}$ (kJ mol <sup>-1</sup> )	57.1	72.3	76.4	73.5	70.0
$\Delta H_{\text{sub}}^T$ (kJ mol <sup>-1</sup> )	$124.2 \pm 0.9$	$137.4 \pm 1.9$	$137.3 \pm 1.8$	$141.7 \pm 1.5$	$124.2 \pm 1.3$
$\Delta H_{\text{sub}}^{298}$ (kJ mol <sup>-1</sup> )	$126.8 \pm 0.9$	$142.8 \pm 1.9$	$144.6 \pm 1.8$	$147.2 \pm 1.5$	$130.4 \pm 1.3$
$C_{p,\text{cr}}^{298}$ (J mol <sup>-1</sup> K <sup>-1</sup> ) <sup>a</sup>	327.5	363.5	340.3	390.1	363.2
$T\Delta S_{\text{sub}}^{298}$ (kJ mol <sup>-1</sup> )	69.7	70.5	68.2	73.7	60.4
$\Delta S_{\text{sub}}^{298}$ (J mol <sup>-1</sup> K <sup>-1</sup> )	$234 \pm 6$	$236 \pm 8$	$229 \pm 7$	$247 \pm 7$	$203 \pm 6$
$\varsigma_H$ (%) <sup>b</sup>	69.0	66.9	68.0	66.6	68.3
$\varsigma_{TS}$ (%) <sup>b</sup>	31.0	33.1	32.0	33.4	31.7
$T_m$ (K)	$371.8 \pm 0.2$	$461.0 \pm 0.2$	$477.6 \pm 0.2$	$403.9 \pm 0.2$	$448.4 \pm 0.2$
$\Delta H_{\text{fus}}^T$ (kJ mol <sup>-1</sup> )	$22.3 \pm 0.5$	$39.6 \pm 0.5$	$45.6 \pm 0.5$	$30.7 \pm 0.5$	$32.4 \pm 0.5$
$\Delta H_{\text{fus}}^{298}$ (kJ mol <sup>-1</sup> )	17.9	25.6	28.5	22.7	21.5
$\Delta S_{\text{fus}}^T$ (J mol <sup>-1</sup> K <sup>-1</sup> ) <sup>c</sup>	60.0	85.9	95.5	76.0	72.3

<sup>a</sup> $C_{p,\text{cr}}^{298}$  has been calculated by Chikcos additive scheme;<sup>40</sup> the error of the calculation procedure corresponds to a significant digit. <sup>b</sup> $\varsigma_H = [\Delta H_{\text{sub}}^{298} / (\Delta H_{\text{sub}}^{298} + T\Delta S_{\text{sub}}^{298})] \cdot 100\%$ ;  $\varsigma_{TS} = [T\Delta S_{\text{sub}}^{298} / (\Delta H_{\text{sub}}^{298} + T\Delta S_{\text{sub}}^{298})] \cdot 100\%$ . <sup>c</sup> $\Delta S_{\text{fus}}^T = \Delta H_{\text{fus}}^T / T_m$

occurring in crystals during sublimation and fusion is different. For example, such effects as vacancies (i.e., free volume) are responsible for «stepwise mechanism» of sublimation of molecular crystals.<sup>62</sup> In this context, we analyzed the way  $V^{\text{free}}$  influences thermodynamic functions. If we want to study the effect of molecule topology on crystal package architecture and thermodynamic characteristics respectively, we are to analyze the  $\beta$ -parameter (or  $D_{\text{cal}}$ ). A considerable change in molecule conformation during crystal lattice formation results in a nonadditive increase in the free volume per molecule in a crystal with the van der Waals volume increasing.  $V^{\text{vdw}}$  is to be used to analyze the effect of the molecule size only on the processes under study. One can trace how much the molecule topology influences the way the molecule is packed in a crystal by analyzing experimental values by plotting  $\beta$  versus  $V^{\text{vdw}}$  (Figure 11). One cannot but see that the compounds with approximately equal van der Waals volumes possess different package density values (I and III and V and VI). Adding substituents into the phenyl ring of compound XIV causes

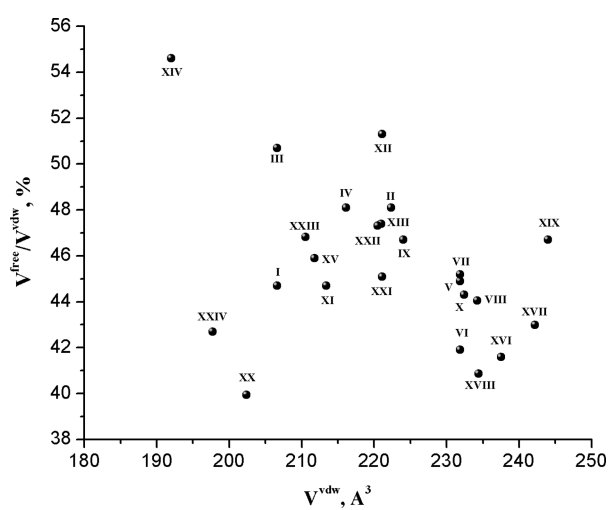


**Figure 11.** Plot of  $V^{\text{free}}/V^{\text{vdw}}$  vs  $V^{\text{vdw}}$  for the compounds studied.

package density of the molecules in a crystal to grow ( $\beta$  value diminishes).

As the  $D_{\text{cal}}$  parameter is an entropy characteristic of a crystal, we attempted to compare these values with the entropy terms of sublimation  $T\Delta S_{\text{sub}}^{298}$  of the compounds under study (in the way similar to that described in our previous work<sup>31</sup>). It must be noted that thermodynamic characteristics of sublimation for some compounds (indicated by red) drop out of correlation dependences with  $D_{\text{cal}}$ , which may be ascribed to a considerable difference in the ratio of various contributions of the interactions between the molecules in crystal lattices as contrasted to the substances for which the given correlation is observed. Figure 12 presents the experimental values. For the

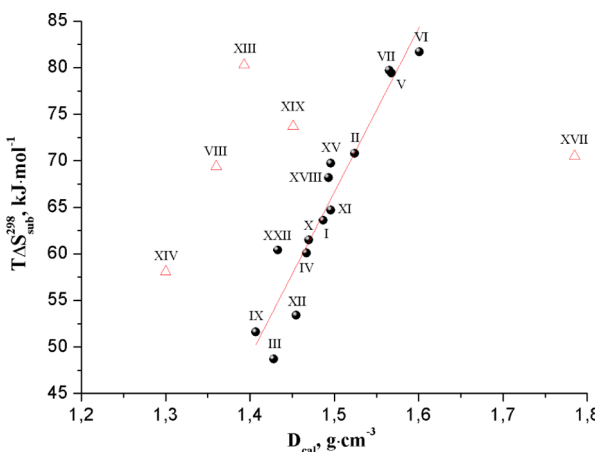


**Figure 12.** Correlation between the sublimation entropic terms ( $T\Delta S_{\text{sub}}^{298}$ ) and the calculated molecular densities ( $D_{\text{cal}}$ ) in the crystal lattices (numbering corresponds to Figure 1).

compounds indicated by the black color, these may be described by the following correlation equation:

$$T\Delta S_{\text{sub}}^{298} = (-198 \pm 24) + (176 \pm 16)D_{\text{cal}} \quad (7)$$

$$r = 0.955; \sigma = 3.21; F = 124.3; n = 14$$

It can be assumed that the experimentally derived density values will correlate with the calculated ones. Therefore, no

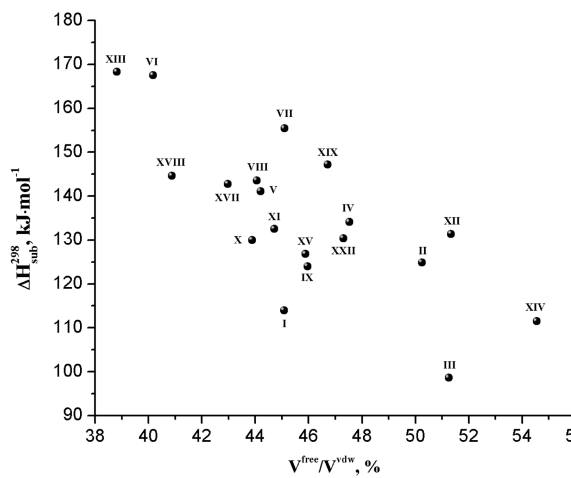
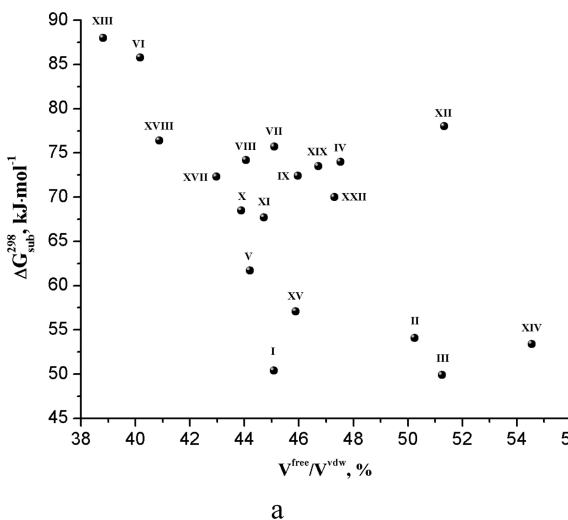
additional information about crystal structure is required to evaluate the sublimation entropy member directly from experimental density values.

Figure 13 shows the experimental thermodynamic functions ( $\Delta G_{\text{sub}}^{298}$  and  $\Delta H_{\text{sub}}^{298}$ ) versus the molecular package density in the crystals investigated. One cannot help but notice comparable tendencies in their behavior: the increase in the  $\beta$  parameter (i.e., diminishing in molecular package density) results in a lowering of the Gibbs energy and sublimation enthalpy values. Of course, there is some spread in values which may be attributed to the great difference of hydrogen bond network topology and structures.

It is a well-known fact that temperature and enthalpy of crystal fusion are often used in pharmaceutics as parameters describing (simulating) the crystal lattice. It can be exemplified by the equation of solubility derived by Yalkowsky.<sup>63</sup> The wide recognition of these parameters is associated with the fact that they are experimentally trivial and can be obtained by means of conventional techniques of DSC experiments. The nature and mechanisms responsible for fusion temperature values are still under discussion in the literature.<sup>57</sup> We attempted to find out correlations between these temperatures and contributions of nonbonded van der Waals interactions between various SA fragments (included previously) to packing energy.

There is a satisfactory (approximately linear) correlation between  $T_m$  and  $E^{4-4}$  for chlorine-containing sulfonamides: the growth of interaction energy between the second phenyl fragments of adjacent molecules makes the temperature of fusion also rise (Figure 14). As was mentioned above, the contribution of  $E^{4-4}$  to the packing energy is maximal for all the investigated compounds in contrast to other contributions. Hence, one can assume that the process of fusion begins with the loss of contacts between the second phenyl fragments of SA.

The analysis of enthalpies of fusion has revealed that this thermophysical function is influenced by van der Waals interactions between the second phenyl rings. As is shown in Figure 15, the growth of the  $E^{4-4}$  contribution results in growing of fusion enthalpy, this tendency being observed for the following groups of compounds: chlorine derivatives (indicated in red) and para-substituted sulfonamides (indicated in blue).



**Figure 13.** Plots of (a)  $\Delta G_{\text{sub}}^{298}$  vs  $V^{\text{free}}/V^{\text{vdw}}$  and (b)  $\Delta H_{\text{sub}}^{298}$  vs  $V^{\text{free}}/V^{\text{vdw}}$  for the compounds studied (numbering corresponds to Figure 1).

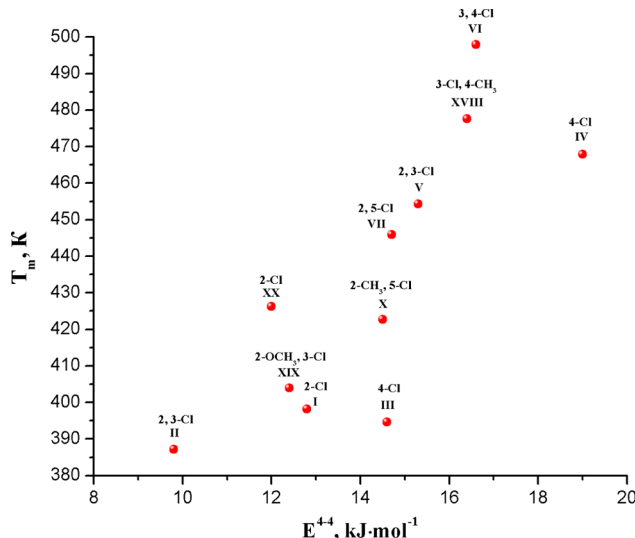


**Figure 14.** Relationship between the melting points and  $E^{4-4}$  contributions in the packing energy made by the nonbonded van der Waals interactions.

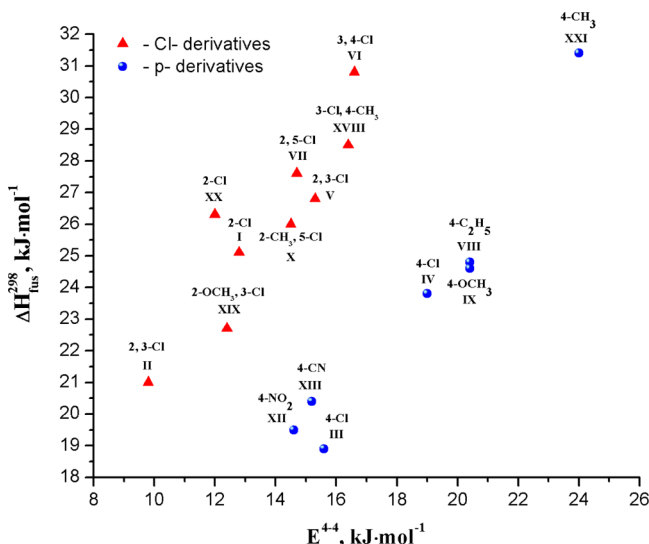


**Figure 15.** Relationship between  $\Delta H_{\text{sub}}^{298}$  and  $E^{4-4}$  contributions in the packing energy made by the nonbonded van der Waals interactions.

It should be emphasized, that there is a correlation between the Gibbs energy of sublimation and the temperature of fusion for the investigated compounds (Figure 16). In view of the fact that it is easy to determine thermophysical characteristics of fusion processes by means of DSC experiments, correlation equations become an adequate means of evaluating thermodynamic parameters of sublimation.

## CONCLUSION

The crystal structures of ten sulfonamides (XV–XXIV) have been solved by X-ray diffraction experiments. Comparative analysis of molecular conformational states has been carried out. One can observe a favorable correlation between  $\tau_3$  and  $\angle \text{Ph1–Ph2}$ . Therefore, the  $\tau_3$  angle appears to be the most susceptible to structural SA molecule modifications and makes the main contribution to the turn between the two phenyl rings.

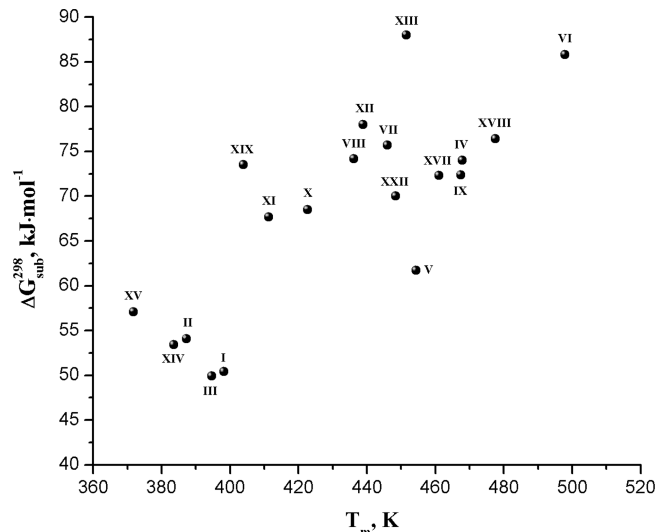


**Figure 16.** Relationship between the sublimation Gibbs energies ( $\Delta G_{\text{sub}}^{298}$ ) and melting points of the compounds studied (numbering corresponds to Figure 1).

The influence of various molecular fragments on the crystal packing energy was analyzed. When handling para-amino-derivatives of sulfonamides in the first phenyl ring (Ph1) and two substituents in the second one (Ph2), the following regularities have been deduced. For SA with a much denser molecular packing in a crystal, the main contributions to stabilizing crystal lattice conform to the interactions between comparable phenyl fragments (Ph1–Ph1 and Ph2–Ph2) of adjacent molecules. As for compounds with lower density packing, it is the bridge connecting two aromatic rings that interfere in energy distribution, Ph2–Ph2, and Ph1–Bridge.

Groups into which all the compounds under study were conditionally subdivided according to their molecular packing in a crystal were analyzed and compared with the basic fragment contributions to crystal lattice energy stabilization. It has been discovered that for the compounds of group I, the main contributions to energy stabilization are produced by the interactions between the first and the second phenyl rings as well as those between the bridge and the second phenyl fragments of the adjacent molecules. For group II sulfonamides, the basic contributions are made, in their turn, by the interactions between the second phenyl rings and those between the first ring and the bridge. Prevailing contributions to crystal lattice energy for the compounds of group III are the interactions between identical phenyl rings of the adjacent molecules.

The thermodynamic aspects of the sulfonamide sublimation processes have been studied by investigating the temperature dependence of vapor pressure by the transpiration method. A regression equation was derived describing the correlation between the sublimation entropy terms and the crystal density data calculated by the X-ray diffraction results.

A quite satisfactory correlation between  $T_m$  and  $E^{4-4}$  is observed for chlorine-containing sulfonamides: the increase in interaction energy between the second phenyl fragment of adjacent molecules raises the temperature of fusion. As it has been demonstrated above,  $E^{4-4}$  contribution to packing energy is maximal for practically all the investigated compounds, in contrast to other contributions. That is why one can assume that the process of fusion begins with the loss of contact

702 between the second SA phenyl fragments. Correlations have  
 703 been established between Gibbs energy of sublimation and  
 704 fusion temperature of the investigated compounds.

## 705 ■ ASSOCIATED CONTENT

### 706 ■ Supporting Information

707 CIF files of the XV–XXIV compounds, some parameters  
 708 describing molecular conformational states in the crystal  
 709 lattices, structural formulas and ref. codes of the crystal  
 710 structures used from the literature, hydrogen bond geometry  
 711 and graph set notations of the molecules studied, hydrogen  
 712 bond geometry and graph set notations of the molecules  
 713 studied, temperature dependencies of saturation vapor pressure  
 714 of the compounds studied, plots of  $V^{\text{free}}/V^{\text{vdw}}$  versus  $V^{\text{vdw}}$  and  
 715  $V^{\text{free}}$  versus  $V^{\text{vdw}}$ , frequency of occurrence of different  
 716 topological graphs of the second level for SA studied, some  
 717 figures illustrated molecular packing in the crystal lattices  
 718 considered. This material is available free of charge via the  
 719 Internet at <http://pubs.acs.org.org>.

## 720 ■ AUTHOR INFORMATION

### 721 Corresponding Author

722 \*E-mail: glp@isc-ras.ru. Tel: +7-4932-533784. Fax: +7-4932-  
 723 336237.

### 724 Notes

725 The authors declare no competing financial interest.

## 726 ■ ACKNOWLEDGMENTS

727 This work was supported by the Russian Foundation of Basic  
 728 Research (Grant 12-03-00019) and the International Science &  
 729 Technology Centre (Projects #888 and 3777). We would like  
 730 to thank V.P. Kazachenko for assistance in preparation of some  
 731 single crystals.

## 732 ■ REFERENCES

- 733 (1) Owa, T.; Nagasu, T. *Exp. Opin. Ther. Pat.* **2000**, *10*, 1725–1740.
- 734 (2) Abbate, F.; Supuran, C. T.; Scozzafava, A.; Orioli, P.; Stubbs, M.  
 735 T.; Klebe, G. *J. Med. Chem.* **2002**, *45*, 3583.
- 736 (3) Scozzafava, A.; Owa, T.; Mastrolorenzo, A.; Supuran, C. T. *Curr.  
 737 Med. Chem.* **2003**, *10*, 925–953.
- 738 (4) Supuran, C. T.; Scozzafava, A. *Exp. Opin. Ther. Pat.* **2000**, *10*,  
 739 575.
- 740 (5) Sehgelmeble, F.; Janson, J.; Ray, C.; Rosqvist, S.; Gustavsson, S.;  
 741 Nilsson, L. I.; Minidis, A.; Holenz, J.; Rotticci, D.; Lundkvist, J.;  
 742 Arvidsson, P. I. *ChemMedChem* **2012**, *7*, 396–399.
- 743 (6) Thakur, M.; Thakur, A.; Kkadikar, P. V.; Supuran, C. T. *Bioorg.  
 744 Med. Chem. Lett.* **2005**, *15*, 203–209.
- 745 (7) Fujita, T.; Hansch, C. *J. Med. Chem.* **1967**, *10*, 991–1000.
- 746 (8) Bell, P. H.; Roblin, R. O., Jr. *J. Am. Chem. Soc.* **1942**, *64*, 2905–  
 747 2917.
- 748 (9) Hansch, C. *Il Farmaco* **2003**, *58*, 625–629.
- 749 (10) Sethi, K. K.; Saurabh, M. V.; Prasanthi, N.; Sahoo, S. K.; Parhi,  
 750 R. B.; Suresh, P. *Bioorg. Med. Chem. Lett.* **2010**, *20*, 3089–3093.
- 751 (11) Krystek, S. R., Jr.; Hunt, J. T.; Stein, P. D.; Stouch, T. R. *J. Med.  
 752 Chem.* **1995**, *38*, 659–668.
- 753 (12) Stein, P. D.; Floyd, D. M.; Bisaha, S.; Dickey, J.; Girotra, N. R.;  
 754 Gougoutas, J. Z.; Kozlowsky, M.; Lee, V. G.; Liu, E. C.-K.; Malley, M.  
 755 F.; McMullen, D.; Mitchell, C.; Moreland, S.; Murugesan, N.; Serafino,  
 756 R.; Webb, M. L.; Zhang, R.; Hunt, J. T. *J. Med. Chem.* **1995**, *38*, 1344–  
 757 1354.
- 758 (13) Senger, S.; Convery, M. A.; Chan, C.; Watson, N. S. *Bioorg. Med.  
 759 Chem. Lett.* **2006**, *16*, 5731–5735.
- 760 (14) Senger, S.; Chan, C.; Convery, M. A.; Hubbard, J. A.; Shah, G.;  
 761 Watson, N. S.; Young, R. *J. Med. Chem. Lett.* **2007**, *17*, 2931–2934.
- 762 (15) Parkin, A.; Collins, A.; Gilmore, C. J.; Wilson, C. C. *Acta Crystallogr.* **2008**, *B64*, 66–71.
- 763 (16) Brameld, K. A.; Kuhn, B.; Reuter, D. C.; Stahl, M. *J. Chem. Inf. Model.* **2008**, *48*, 1–24.
- 765 (17) Bock, H.; Nagel, N.; Naether, C. *Z. Naturforsch., B: J. Chem. Sci.* **1998**, *53*, 1389–1400.
- 767 (18) Sanphui, P.; Sarma, B.; Nangia, A. *Cryst. Growth Des.* **2010**, *10*, 768 4550–4564.
- 769 (19) Terada, S.; Katagiri, K.; Masu, H.; Danjo, H.; Sei, Y.; Kawahata, M.;  
 770 Tominaga, M.; Yamaguchi, K.; Azumaya, I. *Cryst. Growth Des.* **2012**, *12*, 2908–2916.
- 772 (20) Katagiri, K.; Ikeda, T.; Tominaga, H.; Masu, H.; Azumaya, I. *Cryst. Growth Des.* **2010**, *10*, 2291–2297.
- 774 (21) Zoppi, A.; Quevedo, M. A.; Derlivo, A.; Longhi, M. R. *J. Pharm. Sci.* **2010**, *99*, 3166–3176.
- 776 (22) de Araújo, M. V. G.; Vieira, E. K. B.; Lázaro, G. S.; Conegero, L. S.; Almeida, L. E.; Barreto, L. S.; da Costa, N. B.; Gimenez, Jr.; Gimenez, I. F. *Bioorg. Med. Chem.* **2008**, *16*, 5788–5794.
- 779 (23) Caira, M. R. *Mol. Pharmaceutics* **2007**, *4*, 310–316.
- 780 (24) Goud, N. R.; Gangavaram, S.; Suresh, K.; Pal, S.; Manjunatha, S. G.; Nambiar, S.; Nangia, A. *J. Pharm. Sci.* **2012**, *101*, 664–680.
- 782 (25) Ghosh, S.; Bag, P. P.; Reddy, C. M. *Cryst. Growth Des.* **2011**, *11*, 783 3489–3503.
- 784 (26) Bingham, A. L.; Hughes, D. S.; Hursthause, M. B.; Lancaster, R. W.; Tavener, S.; Threlfall, T. L. *Chem. Commun. (Cambridge, U.K.)* **2001**, 785 603–604.
- 786 (27) Aitipamula, S.; Chow, P. S.; Tan, R. B. H. *CrystEngComm* **2012**, *14*, 788 691–699.
- 789 (28) Pratt, J.; Hutchinson, J.; Stevens, Ch.L.K. *Acta Crystallogr.* **2011**, *C67*, 790 o487–o491.
- 791 (29) Hu, Z.-Q.; Chen, Ch.-F. *Chem. Commun. (Cambridge, U.K.)* **2005**, 792 2445–2447.
- 793 (30) Perlovich, G. L.; Strakhova, N. N.; Kazachenko, V. P.; Volkova, T. V.; Tkachev, V. V.; Schaper, K.-J.; Raevsky, O. A. *Int. J. Pharm.* **2007**, *334*, 115–124.
- 796 (31) Perlovich, G. L.; Strakhova, N. N.; Kazachenko, V. P.; Volkova, T. V.; Tkachev, V. V.; Schaper, K.-J.; Raevsky, O. A. *Int. J. Pharm.* **2008**, *349*, 300–313.
- 799 (32) Perlovich, G. L.; Tkachev, V. V.; Strakhova, N. N.; Kazachenko, V. P.; Volkova, T. V.; Surov, O. V.; Schaper, K.-J.; Raevsky, O. A. *J. Pharm. Sci.* **2009**, *98*, 4738–4755.
- 802 (33) Perlovich, G. L.; Ryzhakov, A. M.; Strakhova, N. N.; Kazachenko, V. P.; Schaper, K.-J.; Raevsky, O. A. *J. Chem. Thermodyn.* **2011**, *43*, 683–689.
- 805 (34) Perlovich, G. L.; Ryzhakov, A. M.; Tkachev, V. V.; Hansen, L. Kr. *Cryst. Growth Des.* **2011**, *11*, 1067–1081.
- 807 (35) Guillory, J. K. *Polymorphism in Pharmaceutical Solids*; Brittain, H. G., Ed.; Marcel Dekker Inc.: New York, 1999; pp 183–226.
- 809 (36) CAD-4 Software, version 5.0; Enraf-Nonius: Delft, The Netherlands, 1989.
- 811 (37) Sheldrick, G. M. *SHELXL97 and SHELXS97*; University of Göttingen: Germany, 1997.
- 813 (38) Zielenkiewicz, W.; Perlovich, G.; Wszelaka-Rylik, M. *J. Therm. Anal. Calorim.* **1999**, *57*, 225–234.
- 815 (39) Cox, J. D.; Pilcher, G. *Thermochemistry of Organic and Organometallic Compounds*; Academic Press: London, 1970.
- 817 (40) Chickos, J. S.; Acree, W. E., Jr. *J. Phys. Chem. Ref. Data* **2002**, *31*, 818 537–698.
- 819 (41) Dannenfelser, R.-M.; Yalkowsky, S. H. *J. Pharm. Sci.* **1999**, *88*, 820 722–724.
- 821 (42) Pascual-Ahuir, J. L.; Silla, E. *J. Comput. Chem.* **1990**, *11*, 1047.
- 822 (43) Gavezzotti, A.; Filippini, G. *Energetic Aspects of Crystal Packing: Experiment and Computer Simulations*. In *Theoretical Aspects and Computer Modeling of the Molecular Solid State*; Gavezzotti, A., Ed.; John Wiley & Sons: Chichester, West Sussex, U.K., 1997; Chapter 3, pp 61–97.
- 827 (44) Alleaume, M.; Dkap, J. *Acta Crystallogr.* **1965**, *18*, 731–736.
- 828 (45) Shefter, E.; Sackman, P. *J. Pharm. Sci.* **1971**, *60*, 282–286.
- 829

- 830 (46) Kalman, A.; Czugler, M.; Argay, G. *Acta Crystallogr.* **1981**, *B37*,  
831 868–877.  
832 (47) Krueger, G. J.; Gafner, G. *Acta Crystallogr.* **1971**, *B27*, 326–333.  
833 (48) Krueger, G. J.; Gafner, G. *Acta Crystallogr.* **1972**, *B28*, 272–283.  
834 (49) Alleaume, M.; Gulkos, A.; Herbstein, F. H.; KaDon, M.; Marsh,  
835 R. E. *Acta Crystallogr.* **1976**, *B32*, 669–682.  
836 (50) Bar, I.; Bernstein, J. J. *Pharm. Sci.* **1985**, *74*, 255–263.  
837 (51) Etter, M. C. *Acc. Chem. Res.* **1990**, *23*, 120–126.  
838 (52) Bernstein, J.; Davis, R. E.; Shimon, L.; Chang, N.-L. *Angew. Chem., Int. Ed. Engl.* **1995**, *34*, 1555–1573.  
839 (53) Perlovich, G. L.; Rodionov, S. V.; Bauer-Brandl, A. *Eur. J. Pharm. Sci.* **2005**, *24*, 25–33.  
840 (54) Gavezzotti, A.; Filippini, G. *J. Am. Chem. Soc.* **1995**, *117*,  
841 12299–12305.  
842 (55) Gavezzotti, A. *J. Am. Chem. Soc.* **2000**, *122*, 10724–10725.  
843 (56) Osborn, J. C.; York, P. *J. Mol. Struct.* **1999**, *474*, 43–47.  
844 (57) Li, Z. J.; Ojala, W. H.; Grant, D. J. W. *J. Pharm. Sci.* **2001**, *90*,  
845 1523–1539.  
846 (58) Kitagorodsky, A. I. *Molecular Crystals and Molecules*; Academic  
847 Press, Inc.: New York, 1973.  
848 (59) Perlovich, G. L.; Proshin, A. N.; Volkova, T. V.; Cong, T. B.;  
849 Bachurin, S. O. *Mol. Pharm.* **2011**, *8*, 1807–1820.  
850 (60) Perlovich, G. L.; Volkova, T. V.; Proshin, A. N.; Sergeev, D.Yu.;  
851 Cong, T. B.; Petrova, L. N.; Bachurin, S. O. *J. Pharm. Sci.* **2010**, *99*,  
852 3754–3768.  
853 (61) Surov, A. O.; Terekhova, I. V.; Bauer-Brandl, A.; Perlovich, G. L.  
854 *Cryst. Growth Des.* **2009**, *9*, 3265–3272.  
855 (62) Lebedev, Yu. A.; Miroshnichenko, E. A. Heats of Evaporation,  
856 Sublimation and Saturated Vapor Pressure. In *Thermochemistry of  
857 Vaporization of Organic Substances*; Nauka: Moscow, 1981; p 216.  
858 (63) Yalkowsky, S. H.; Valvani, S. C. *J. Pharm. Sci.* **1980**, *69*, 912–  
859 922.  
860 (64) Kuz'mina, L. G.; Struchkov, Y. T.; Peregovodov, A. S.; Kravtsov, D.  
861 N.; Russ, J. *Struct. Chem.* **1984**, *25*, 113–121.  
862 (65) Bruni, B.; Coran, S. A.; Bartolucci, G.; Viara, M. D. *Acta  
863 Crystallogr.* **2010**, *E66*, o2663.  
864 (66) Koo, C. H.; Shin, H. S.; Cho, S. I. *Arch. Pharm. Sci. Res.* **1982**, *5*,  
865 79.  
866 (67) Rambaud, J.; Roques, R.; Alberola, S.; Sabon, F. *Bull. Soc. Chim.  
867 Fr.* **1980**, *56*.  
868 (68) Delley, B. *J. Chem. Phys.* **2000**, *113* (18), 7756–7764.